Version of Record: https://www.sciencedirect.com/science/article/pii/S2451910322002290
Manuscript_f144b07b87765ffec4a881a5f63ab151

# Electrochemical Techniques for Visualizing Photoelectrochemical Processes at the Nanoscale

Chloe L. Tolbert, Declan M. McDonald, and Caleb M. Hill*
Department of Chemistry, University of Wyoming
1000 E. University Ave., Laramie WY, 82071
*caleb.hill@uwyo.edu

## Abstract

Two-dimensional semiconductors (2DSCs) are attractive materials for a variety of applications in electronics, photovoltaics, and catalysis. Despite their promise, it is often unclear how the performance of 2DSCs is influenced by structural defects present in these materials such as atomic vacancies or step-edges. A better fundamental understanding of how such structural features influence the generation and transport of charge carriers in 2DSCs will be critical in the pursuit of improved practical devices moving forward. In this Opinion, we highlight how electrochemistry can be leveraged to reveal fascinating insights into the behavior of 2DSCs. Recent advancements in techniques for mapping the rate of photoelectrochemical processes at 2DSCs are outlined and salient experiments employing these techniques are discussed. We conclude with sharing our perspective on opportunities within this field moving forward.

## 1. Introduction

Two-dimensional semiconductors (2DSCs) continue to gain popularity in fields ranging from optoelectronics to catalysis due to their favorable optical and electronic properties and 2D structures which enable their preparation as ultrathin films.[1-5] Unfortunately, the performance of existing 2DSC-based devices, particularly those fabricated via scalable methods, often fail to meet their expected performance. These failures can be attributed to structural nonidealities, or defects, in ultrathin 2DSCs which are not present in their bulk counterparts. Such defects include atomic vacancies, impurities, step edges, etc. which can function as recombination centers for photogenerated carriers in photovoltaic systems or negatively impact chemical stability.[6-9]

Developing a deeper fundamental understanding of how these different structural defects influence behavior will be critical to improving the performance of 2DSC-based devices moving forward. This understanding is difficult to generate using conventional experimental approaches, however, as defects are often present at very high densities (on the order of $10^7$ $cm^{-2}$ or greater).[10] In response to this challenge, there has been a great deal of recent progress in the development and application of techniques capable of resolving photovoltaic behavior in 2DSCs and related materials with nm-scale resolution, allowing researchers to generate valuable new insights into the fundamental carrier transport and kinetics processes that govern the performance of these systems. This review focuses on recent developments in experimental techniques for visualizing these processes at the nm-scale and their application to advance our understanding of important materials systems in the fields of optoelectronics and catalysis.

## 2. Discussion

### *2.1. Experimental Techniques for Mapping Local Photoelectrochemical Behavior*

The efficiency of an optoelectronic device such as a solar cell depends on several factors including the absorption of light to create mobile charge carriers, the transport of these carriers within the absorbing material, and the extraction of these carriers at selective contacts. Photoelectrochemical methods offer a powerful route to fundamental studies into these processes due to the simplicity of preparing carrier-selective semiconductor liquid junctions. In a photoelectrochemical cell, a semiconducting working electrode is brought into contact with an electrolyte and currents are recorded under illumination. These photocurrents directly reflect the overall rate at which charge carriers are generated and transported to the electrolyte interface as well as the kinetics of heterogeneous charge transfer reactions occurring at the interface.

Conventional photoelectrochemical techniques are employed to characterize macroscopic, $mm^2$-scale electrodes and are thus not capable of resolving how behavior varies locally at individual, nm- to μm-scale structural features. A variety of microscopy techniques can be employed to spatially resolve photoelectrochemical reaction rates, a few of which are illustrated in **Figure 1.**[11] One approach is to exert spatial control over charge carrier generation by utilizing a tightly focused light source for excitation and recording photocurrents as the source is scanned across the sample, a general approach which has been employed extensively in the screening of photocatalyst materials[12-18] and has recently been advanced for high-resolution studies of 2DSCs. Using laser-based sources and high-quality optics, illumination can be confined to diffraction-limited regions with dimensions on the order of 0.5 μm. However, the ultimate spatial resolution achieved will also be influenced by the diffusion of photogenerated carriers within the semiconductor if diffusion lengths are comparable to or greater than the optical diffusion limit.[19]

Alternatively, probe-based methods such as Scanning Electrochemical Microscopy (SECM) or Scanning Electrochemical Cell Microscopy (SECCM) can be employed to locally resolve photoelectrochemical reaction rates within illuminated electrode surfaces. In SECM, an inlaid-disk (tip) electrode is positioned near the sample surface and reaction products are detected locally by driving faradaic reactions at the SECM tip.[19] SECCM achieves high spatial resolution by utilizing an electrolyte-filled pipet to create a miniaturized electrochemical cell at the sample surface.[20] Currents flowing through this cell then directly reflect reaction rates within the small region of the sample in contact with the electrolyte. The resolutions achievable *via* SECM and SECCM are ultimately limited by the size of the probes employed and can thus achieve sub-diffraction limit resolution, with resolutions approaching 10 nm having been reported.[21-24] These probe-based methods can also be combined with local illumination schemes to introduce additional functionality, such as the "through-tip illumination" SECM and "carrier-generation tip-collection" SECCM techniques highlighted below.

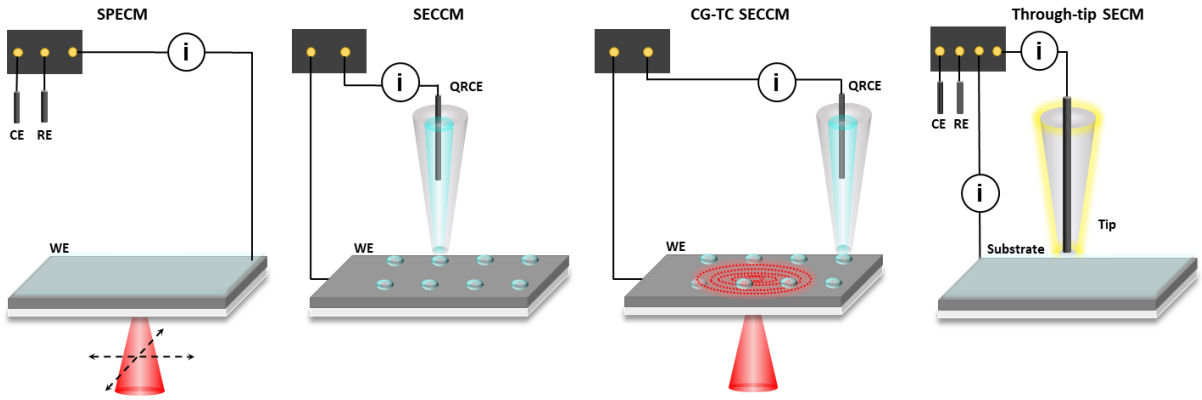


**Figure 1:** Schematic representation of four different electrochemical microscopy techniques.

*2.2. Implementation of Laser Scanning in Photoelectrochemical Approaches*

Sambur and coworkers have reported a series of studies[5, 25-30] which utilize scanning photoelectrochemical microscopy (SPECM) to probe the fundamentals of charge carrier recombination and transport in transition metal dichalcogenides (TMDs), a class of 2DSCs with important potential applications in solar energy harvesting and catalysis. In these experiments, well-defined, μm-scale TMD samples are immobilized on the working electrode of an electrochemical cell and the laser scanning approach illustrated in **Figure 1** is employed to visualize photocurrent generation across these structures. In one study, illustrated in **Figure 2a-f**, photocurrent generation in well-defined monolayer TMD heterojunctions was explored.[28] Using SPECM, photocurrent maps of iodide oxidation at heterojunctions with different stacking configurations (ITO-$MoS_2$-$WS_2$ and ITO-$WS_2$-$MoS_2$) were obtained using different excitation wavelengths (**Figure 2b,c**). For ITO-$MoS_2$-$WS_2$ heterojunctions, strong photocurrents could be observed when employing either 532 nm light (generating carriers in $MoS_2$ and $WS_2$) or 635 nm light (generating carriers selectively in $MoS_2$) for excitation (see **Figure 2e,f**), attributable to the type-II band alignment which drives holes to the electrolyte interface. In ITO-$WS_2$-$MoS_2$ heterostructures, photocurrents were strongly quenched when using 532 nm excitation but, surprisingly, not for 635 nm excitation, revealing an excitation-wavelength-dependent recombination pathway that is characteristic of the TMD stacking orientation. These measurements also revealed that carrier transport occurs over distances on the order of 3 μm despite the facile carrier extraction pathway which is provided via the ultrathin geometry of the monolayer heterostructures. This study highlights the importance of understanding the complex transport and recombination pathways which influence the behavior of bulk heterojunction TMD photoelectrodes.

In a more recent study, SPECM was utilized to reveal doping heterogeneities which can exist within individual TMD nanoflakes.[30] Such heterogeneities can be detrimental to the performance of bulk heterojunction devices, as opposing photocurrents are generated in different areas of a material to effectively cancel out. Here, the stoichiometry and morphology of exfoliated $MoS_2$ nanoflakes were characterized by XPS, ICP-AES, and SEM-EDS. Single nanoflake SPECM measurements of both natural and synthetically-doped $MoS_2$ crystals revealed distinct n- and p-type domains in the same nanoflake (**Figure 2g,h**). The currents produced within individual n- and p-domains (iodide oxidation and triiodide reduction, respectively) effectively cancel each other out due to the additive nature of photocurrents, leading to a

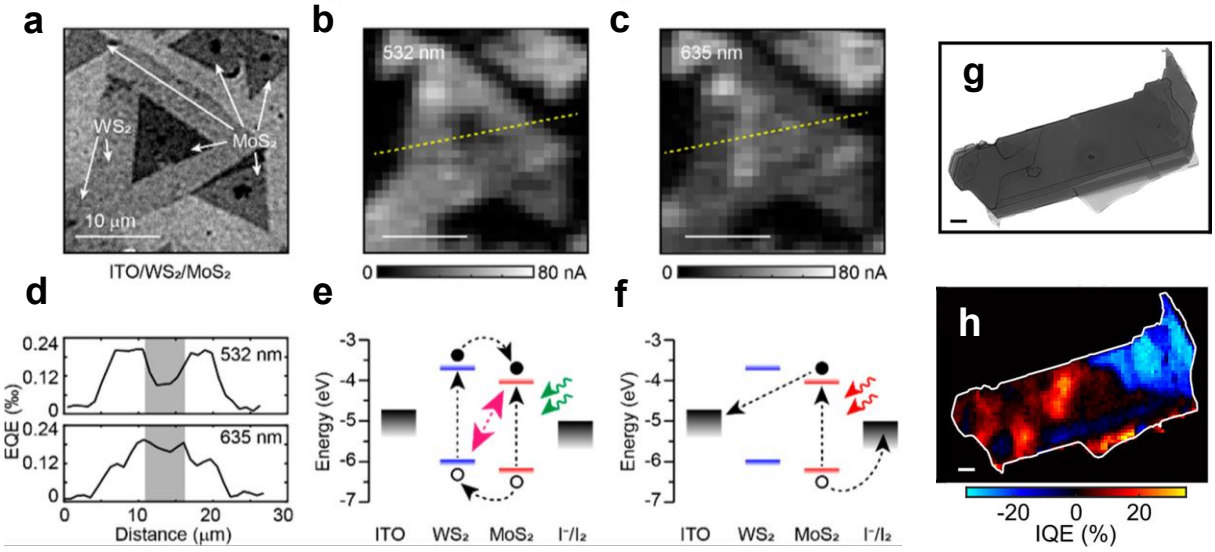


**Figure 1**: Adapted from references 28 and 30. Charge carrier transport and recombination pathways under both green and red illumination conditions. (a) Optical transmission image of the ITO/$MoS_2$/$WS_2$ sample. (b,c) Photocurrent maps under (b) 13.5 kW/cm$^2$ 532 nm laser excitation and (c) 5.7 kW/cm$^2$ 635 nm laser excitation. (d) EQE versus the distance line profile measured from the yellow lines in panels b and c. (e,f) Schematic energy level diagram and proposed charge recombination and transport pathways in the heterojunction region under green and red laser illumination, respectively. (g) Bright-field transmission image of a 63 nm thick natural $MoS_2$ flake and (h) corresponding IQE map.

decrease in overall performance. These SPECM studies reveal doping heterogeneities likely contribute to the discrepancies observed between the bulk and nanoscale photoelectrochemical performance of TMD materials, but these heterogeneities may also enable new approaches to the design of photocatalysts which naturally incorporate later p-n heterojunctions.

### *2.3. SECCM as a Tool for Visualizing Photoelectrochemical Processes*

SECCM has emerged as a powerful tool for the study of electrochemical processes at heterogeneous interfaces and has provided valuable new insights into novel electrocatalysts[22, 31, 32], ion transport membranes[33], and fundamental electrochemical kinetics.[34, 35] In recent years, Hill and coworkers have advanced the use of SECCM for the visualization of photoelectrochemical processes in 2DSCs.[18, 36-39] In this context, SECCM can be utilized to essentially create miniaturized photoelectrochemical interfaces with nm- to μm-scale dimensions which can be characterized to reveal how structural features within these interfaces influence photoelectrochemical behavior. An example is shown in **Figure 3**, where SECCM was employed to map the photoelectrochemical reduction of $Ru(NH_3)_6^{3+}$ across exfoliated p-type $WSe_2$ nanosheets. The use of SECCM allows the behavior of pristine basal planes to be distinguished from different types of defect structures like the step-edge defect present in the $WSe_2$ nanosheet in **Figure 3**. In this example, the p-$WSe_2$ basal planes produce strong photocathodic currents as expected whereas step-edge defects are found to exhibit poor photocathodic currents and can enable photocorrosion at anodic potentials. However, SECCM studies have also revealed that

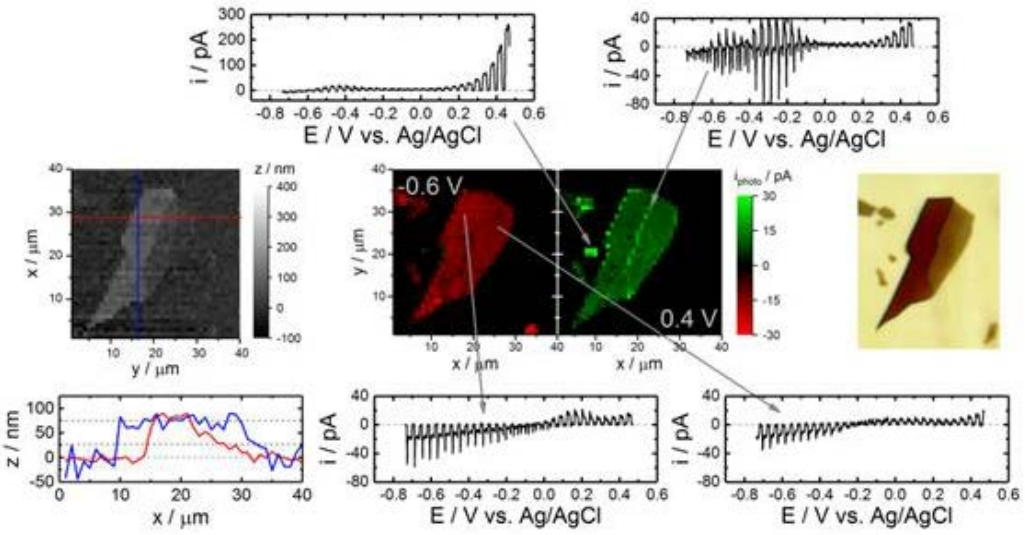


**Figure 3:** Mapping the photoelectrochemical behavior of p-type $WSe_2$ nanosheets via SECCM. Photocurrent images of an exfoliated nanosheet supported on indium tin oxide (optical transmission image given to the right) were constructed from voltammograms taken at 1 µm spatial increments. The pipet was filled with an aqueous electrolyte solution containing 25 mM citric acid, 25 mM trisodium citrate, and 10 mM $Ru(NH_3)_6Cl_3$. Picture adapted with permission from reference 40.

shorter step-edge features can be beneficial for driving inner-sphere processes at TMD materials.[38-40] More recently, this approach has been applied to map the photoelectrochemical behavior of vertical $WSe_2/WS_2$ heterostructures, revealing how photocurrents vary in these systems as a function of thickness and stacking order.[36] Transitioning from bulk TMD nanoflakes to monolayer yields intriguing properties, such as an enhanced molar absorption coefficient, switch from indirect to direct bandgap, and long-range photogenerated carrier transport.[41-44]

In the SECCM studies described above, samples are evenly illuminated over wide areas which means the resulting data reflects local variations in reaction kinetics, charge separation, or carrier recombination. Recently, the carrier generation-tip collection (CG-TC) mode of SECCM has been demonstrated as a tool to selectively map carrier transport in complex 2DSC structures. In CG-TC SECCM, a tightly-focused laser is utilized to locally generate carriers within a sample of interest. Carriers generated within the illuminated region diffuse outwards and those which reach a pipet-based probe positioned some distance away are able to drive a redox reaction at the electrolyte interface, giving rise to a measurable photocurrent. By analyzing these photocurrents as a function of probe position, carrier transport can be directly visualized and quantitative insights into carrier diffusion and recombination can be generated. In initial experiments, CG-TC SECCM was applied to visualize transport in bulk $WSe_2$ nanoflakes, both within pristine basal planes as well as well-defined step-edge features. Within basal planes, bulk in-plane and out-of-plane diffusion lengths were measured to be ~3 µm and ~6 nm, respectively. CG-TC measurements also revealed that individual step-edge defects could act to completely suppress lateral carrier transport (**Figure 4a,b**). These results suggest that strong fields exist within these materials that actively drive carriers toward these defects, effectively enhancing the local carrier recombination rate. CG-TC SECCM studies have since been extended to few-layer $WSe_2$

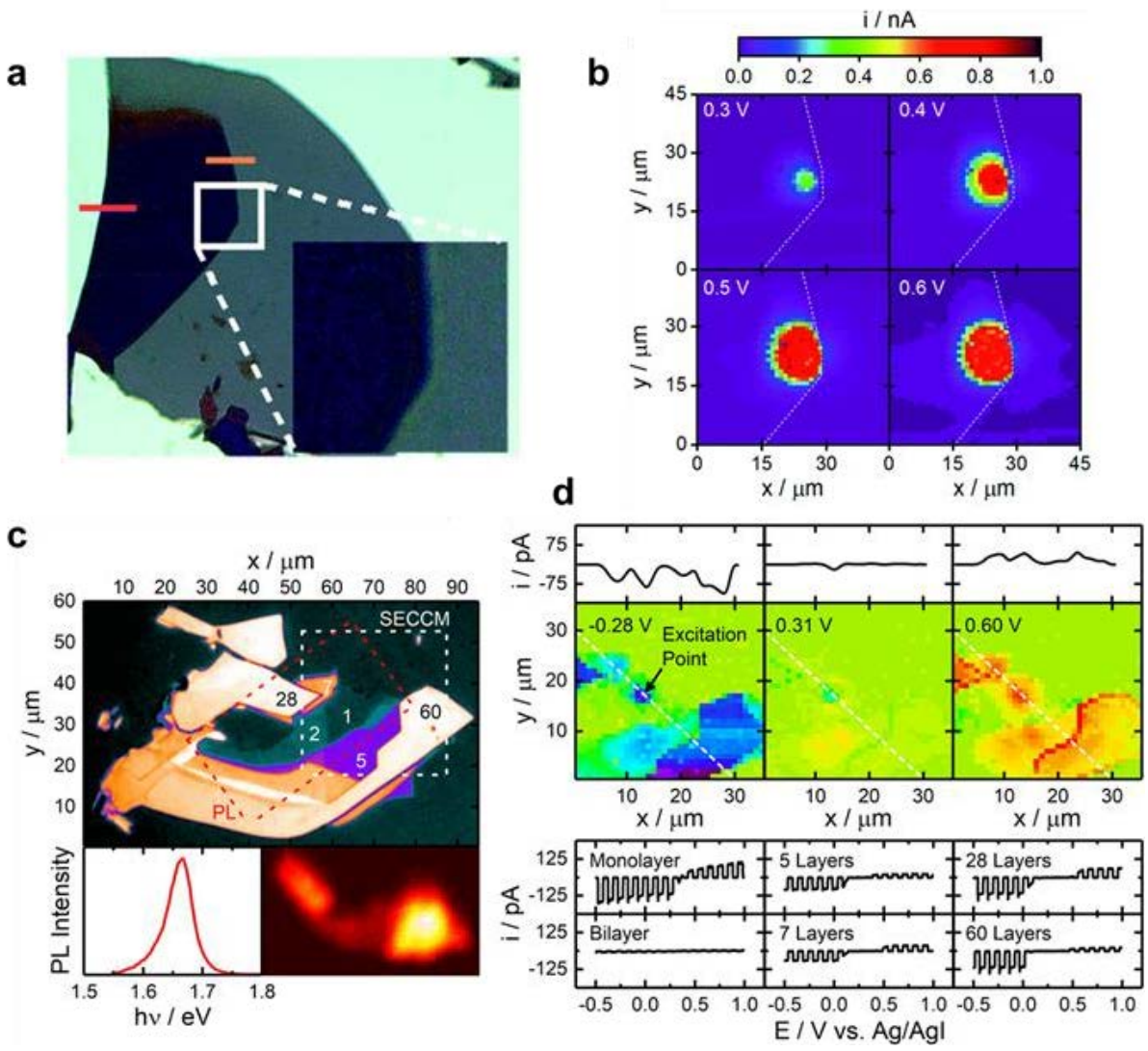


**Figure 4**: Adapted from references 18 and 37. CG-TC SECCM studies of $WSe_2$ nanoflakes. (a) optical transmission image of a multilayered bulk $WSe_2$ nanoflake. The orange line corresponds to a step-edge height of 64 nm and the red line corresponds to a step-edge height of 94 nm from the ITO substrate to the sample. (b) Photocurrent mapping images of the sample in (a) at a series of different applied potentials (1 µm resolution). (c) False color optical reflection and photoluminescence (PL) images of an exfoliated $WSe_2$ structure. The number of $WSe_2$ layers in different regions established via AFM measurements are indicated. A PL spectrum acquired from the monolayer is given below. (d) Photocurrent images at different potentials obtained in the vicinity of a chopped (20 Hz) focused 633 nm laser (0.4 µW). Voltammograms obtained at different potentials along the white dashed line are given below.

structures[45], where distinct changes in band structure are known to occur which impact the nature and properties of photogenerated carriers.[41-44]

**Figure 4c** shows a complex $WSe_2$ nanoflake exhibiting a variety of regions with thicknesses down to the monolayer level. CG-TC measurements revealed carriers generated

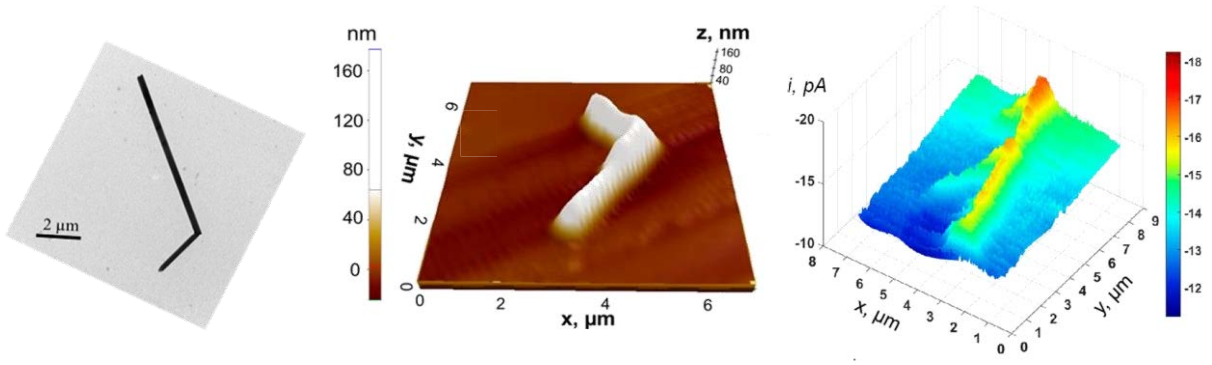


**Figure 5:** (a) TEM image of a $TiO_2$ nanorod supported on an Au TEM grid. (b) Noncontact mode topographic AFM image of the same nanorod. (c) A photo-SECM map of photoelectrochemical oxygen evolution obtained under through-tip UV illumination (200 W HgXe lamp). Data obtained in a 0.1 M borate buffer (pH 8.5) in 0.5 M $Na_2SO_4$. Adapted with permission from reference 49.

within the monolayer region could drive photocurrents at distances greater than 20 µm away. Photocurrents observed in bilayer regions were negligible compared to other sample areas. (**Figure 4d**), attributable to electrostatic forces caused by the formation of interlayer excitons in the bilayer region. Together, these studies offer new insights into carrier transport and recombination at the nanoscale and the importance of defect mitigation to improve practical 2DSC-based devices.

### *2.4. SECM Techniques for Probing Photoelectrochemistry at Individual Nanostructures*

As the most mature probe-based electrochemical technique, SECM has long been recognized as a useful tool for imaging a wide variety of electrochemical processes, though its application to photoelectrochemical systems is complicated by the need to illuminate the surface of a sample in close proximity to a tip electrode. This problem can be overcome by employing through-tip illumination, wherein excitation light is coupled into the glass sheath of an inlaid disk electrode.[46, 47] Recently, significant improvements to this methodology have been made by Mirkin and coworkers which have enabled SECM studies of photoelectrochemical systems to be carried out effectively at the nanoscale.[48-50] In one example depicted in **Figure 5**, through-tip illumination was combined with the substrate generation-tip collection (SG-TC) mode of SECM to image photoelectrochemical oxygen evolution at individual $TiO_2$ nanorods supported on Au TEM grids. These results demonstrate the potential of SECM, which can provide rich chemical information on the nature of electrochemically active surface sites and identity of reaction products, to be combined to atomic-resolution structural probes to generate unparalleled insights into the factors controlling reactivity in photoelectrochemical systems. Using this approach, SECM could similarly serve as a powerful tool for characterizing the photoelectrochemical behavior of nm-scale features within extended materials such as 2DSCs.

## 3. Conclusions and Outlook

The work highlighted in this review demonstrates how recent experimental developments have provided researchers with the tools to explore the photoelectrochemical behavior of materials at the nanoscale. While valuable insights into carrier transport and recombination pathways in 2DSCs have been produced with these newly developed methods, the work carried out to date in this field is merely scratching the surface. Materials beyond TMDs remain largely unexplored, as do heterostructured photocatalyst systems which will continue to grow in importance moving forward given their potential applications in solar fuel production and $CO_2$ remediation.[51] And while considerable progress has been made in the development of these photoelectrochemical microscopy techniques, further improvements in spatial resolution are needed to "catch up" to modern structural characterization tools such as TEM and enable the chemical behavior of atomic-scale active sites and surface defects in these systems to be elucidated. Moving forward, these nanoscale methods will be critical to improving our understanding of emerging photoelectrochemical systems.

## Acknowledgements

The authors would like to acknowledge generous support from the National Science Foundation (CHE-2045593 and OIA-2119237) and the University of Wyoming School of Energy Resources.

## Declaration of interests

The authors declare that they have no known competing financial interests or personal relationships that could have appeared to influence the work reported in this paper.

## References

1. Jariwala, D.; Davoyan, A. R.; Wong, J.; Atwater, H. A., Van der Waals materials for atomically-thin photovoltaics: promise and outlook. *ACS Photonics* **2017,** *4* (12), 2962-2970.
2. Wang, L.; Huang, L.; Tan, W. C.; Feng, X.; Chen, L.; Huang, X.; Ang, K.-W., 2D photovoltaic devices: Progress and prospects. *Small Methods* **2018,** *2* (3).
3. Jariwala, D.; Sangwan, V. K.; Lauhon, L. J.; Marks, T. J.; Hersam, M. C., Emerging device applications for semiconducting two-dimensional transition metal dichalcogenides. *ACS Nano* **2014,** *8* (2), 1102-1120.
4. Sivula, K.; van de Krol, R., Semiconducting materials for photoelectrochemical energy conversion. *Nature Reviews Materials* **2016,** *1*.
5. Wang, L.; Sambur, J. B., Efficient ultrathin liquid junction photovoltaics based on transition metal dichalcogenides. *Nano Letters* **2019,** *19* (5), 2960-2967.
6. Menezes, S.; Schneemeyer, L. F.; Lewerenz, H. J., Efficiency losses from carrier-type inhomogeneity in tungsten diselenide photoelectrodes. *Applied Physics Letters* **1981,** *38*.
7. Yuan, L.; Wang, T.; Zhu, T.; Zhou, M.; Huang, L., Exciton dynamics, transport, and annihilation in atomically thin two-dimensional semiconductors. *Journal of Physical Chemistry Letters* **2017,** *8* (14), 3371-3379.

8. Chen, K.; Roy, A.; Rai, A.; Movva, H. C. P.; Meng, X.; He, F.; Banerjee, S. K.; Wang, Y., Accelerated carrier recombination by grain boundary/edge defects in MBE grown transition metal dichalcogenides. *APL Materials* **2018,** *6* (5).
9. Wang, H.; Zhang, C.; Rana, F., Ultrafast dynamics of defect-assisted electron-hole recombination in monolayer $MoS_2$. *Nano Letters* **2014,** *15* (1), 339-345.
10. Qui, H.; Xu, T.; Wang, Z.; Ren, W.; Nan, H.; Ni, Z.; Chen, Q.; Yuan, S.; Miao, F.; Song, F.; Long, G.; Shi, Y.; Sun, L.; Wang, J.; Wang, X., Hopping transport through defect-induced localized states in molybdenum disulphide. *Nature Communications* **2013,** *4*.
11. Hill, C. M.; Pan, S., SECM Techniques for Locally Interrogating the Photocatalytic Activity of Semiconducting Materials for Solar-Driven Chemical Transformations. In *Scanning Electrochemical Microscopy*, 2022; pp 361-378.
12. Ma, Y.; Shinde, P. S.; Li, X.; Pan, S., High-throughput screening and surface interrogation studies of Au-modified hematite photoanodes by scanning electrochemical microscopy for solar water splitting. *ACS Omega* **2019,** *4* (17), 17257-17268.
13. Shinde, P. S.; Peng, X.; Wang, J.; Ma, Y.; McNamara, L. E.; Hammer, N. I.; Gupta, A.; Pan, S., Rapid screening of photoanode materials using scanning photoelectrochemical microscopy technique and formation of Z-scheme solar water splitting system by coupling p- and n-type heterojunction photoelectrodes. *ACS Applied Energy Materials* **2018,** *1* (5), 2283-2294.
14. Kimmich, D.; Taffa, D. H.; Dosche, C.; Wark, M.; Wittstock, G., Combinatorial screening of photoanode materials - Uniform platform for compositional arrays and macroscopic electrodes. *Electrochimica Acta* **2018,** *259*, 204-212.
15. Skorupska, K.; Parkinson, B. A., Combinatorial synthesis and screening of oxide materials for photoelectrochemical energy conversion. In *Photoelectrochemical Solar Fuel Production*, Gimenez, S.; Bisquert, J., Eds. Springer, Cham.: 2016; pp 427-462.
16. Hsu, H.-Y.; Ji, L.; Du, M.; Zhao, J.; Tu, E. T.; Bard, A. J., Optimization of lead-free organic–inorganic tin(II) halide perovskite semiconductors by scanning electrochemical microscopy. *Electrochimica Acta* **2016,** *220*, 205-210.
17. Skorupska, K.; Maggard, P. A.; Eichberger, R.; Schwarzburg, K.; Shahbazi, P.; Zoellner, B.; Parkinson, B. A., Combinatorial investigations of high temperature CuNb oxide phases for photoelectrochemical water splitting. *ACS Combinatorial Science* **2015,** *17* (12), 742-751.
18.** Hill, J. W.; Hill, C. M., Directly visualizing carrier transport and recombination at individual defects within 2D semiconductors. *Chemical Science* **2021,** *12*, 5102-5112.

This study introduced the concept of CG-TC SECCM and looked at carrier recombination at pristine basal planes and step-edge defects in bulk TMD nanoflakes. In-plane and out-of-plane diffusion lengths were measured at basal planes, and electrochemical "movies" were provided to visualize recombination at step-edge defects.

19. Bard, A. J.; Mirkin, M. V., *Scanning Electrochemical Microscopy*. 3rd ed.; CRC Press: 2022.
20. Snowden, M. E.; Guell, A. G.; Lai, S. C. S.; McKelvey, K.; Ebejer, N.; O'Connell, M. A.; Colburn, A. W.; Unwin, P. R., Scanning electrochemical cell microscopy: Theory and experiment for quantitative high resolution spatially-resolved voltammetry and simultaneous ion-conductance measurements. *Analytical Chemistry* **2012,** *84* (5), 2483-2491.

21. Shigyou, K.; Sun, L.; Yajima, R.; Takigaura, S.; Tajima, M.; Furusho, H.; Kikuchi, Y.; Miyazawa, K.; Fukuma, T.; Taoka, A.; Ando, T.; Watanabe, S., Geometrical characterization of glass nanopipettes with sub-10 nm pore diameter by transmission electron microscopy. *Analytical Chemistry* **2020,** *92* (23), 15388-15393.
22. Bentley, C. L.; Kang, M.; Unwin, P. R., Nanoscale structure dynamics within electrocatalytic materials. *Journal of the American Chemical Society* **2017,** *139* (46), 16813-16821.
23. Sun, T.; Yu, Y.; Zacher, B. J.; Mirkin, M. V., Scanning electrochemical microscopy of individual catalytic nanoparticles. *Angewandte Chemie International Edition* **2014,** *53* (51), 14120-14123.
24. Kim, J.; Renault, C.; Nioradze, N.; Arroyo-Curras, N.; Leonard, K. C.; Bard, A. J., Electrocatalytic activity of individual Pt nanoparticles studied by nanoscale scanning electrochemical microscopy. *Journal of the American Chemical Society* **2016,** *138* (27), 8560-8568.
25. Isenberg, A. E.; Todt, M. A.; Wang, L.; Sambur, J. B., Role of photogenerated iodine on the energy-conversion properties of $MoSe_2$ nanoflake liquid junction photovoltaics. *ACS Applied Materials Interfaces* **2018,** *10* (33), 27780-27786.
26. Todt, M. A.; Isenberg, A. E.; Nanayakkara, S. U.; Miller, E. M.; Sambur, J. B., Single-nanoflake photo-electrochemistry reveals champion and spectator flakes in exfoliated $MoSe_2$ films. *Journal of Physical Chemistry C* **2018,** *122* (12), 6539-6545.
27. Wang, L.; Schmid, M.; Nilsson, Z. N.; Tahir, M.; Chen, H.; Sambur, J. B., Laser annealing improves the photoelectrochemical activity of ultrathin $MoSe_2$ photoelectrodes. *ACS Applied Materials Interfaces* **2019,** *11* (21), 19207-19217.
28.** Wang, L.; Tahir, M.; Chen, H.; Sambur, J. B., Probing charge carrier transport and recombination pathways in monolayer $MoS_2/WS_2$ heterojunction photoelectrodes. *Nano Letters* **2019,** *19* (12), 9084-9094.

Different stacking orientations of monolayered TMD heterojunctions were investigated with SPECM at two different wavelengths: 532 nm which generates carriers in both $WS_2$ and $MoS_2$, and 635 nm which selectively generates carriers in $MoS_2$. This revealed an excitation-wavelength-dependent recombination pathway that is characteristic of the TMD stacking orientation. Diffusion lengths were also measured to be ~ 3 μm, even though a perpendicular carrier extraction pathway is provided via the geometry of the monolayers.

29. Wang, L.; Nilsson, Z. N.; Tahir, M.; Chen, H.; Sambur, J. B., Influence of the substrate on the optical and photoelectrochemical properties of monolayer $MoS_2$. *ACS Applied Materials Interfaces* **2020,** *12* (13), 15034-15042.
30.** Van Erdewyk, M.; Sambur, J. B., Single nanoflake photoelectrochemistry reveals intrananoflake doping heterogeneity that explains ensemble-level photoelectrochemical behavior. *ACS Applied Materials Interfaces* **2022,** *14* (20), 22737-22746.

SPECM allowed for the visualization of distinct p- and n-type regions within the same naturally-doped and synthetically-doped TMD nanosheets. Photocurrents measured from p- and n-type regions effectively cancelled each other out, which could help to explain the low performance of bulk PEC devices.

31. Wahab, O. J.; Kang, M.; Daviddi, E.; Walker, M.; Unwin, P. R., Screening surface structure-electrochemical activity relationships of copper electrodes under $CO_2$ electroreduction conditions. *ACS Catalysis* **2022,** *12* (11), 6578-6588.
32. Mefford, J. T.; Akbashev, A. R.; Kang, M.; Bentley, C. L.; Gent, W. E.; Deng, H. D.; Alsem, D. H.; Yu, Y.-S.; Salmon, N. J.; Shapiro, D. A.; Unwin, P. R.; Chueh, W. C., Correlative operando microscopy of oxygen evolution electrocatalysts. *Nature* **2021,** *593*, 67-73.
33. Bentley, C. L.; Kang, M.; Bukola, S.; Creager, S. E.; Unwin, P. R., High-resolution ion-flux imaging of proton transport through graphene|nafion membranes. *ACS Nano* **2022,** *16* (4), 5233-5245.
34. Liu, D.-Q.; Kang, M.; Perry, D.; Chen, C.-H.; West, G.; Xia, X.; Chaudhuri, S.; Laker, Z. P. L.; Wilson, N. R.; Meloni, G. N.; Melander, M. M.; Maurer, R. J.; Unwin, P. R., Adiabatic versus non-adiabatic electron transfer at 2D electrode materials. *Nature Communications* **2021,** *12*.
35. Yu, Y.; Zhang, K.; Parks, H.; Babar, M.; Carr, S.; Craig, I. M.; Van Winkle, M.; Lyssenko, A.; Taniguci, T.; Watanabe, K.; Viswanathan, V.; Bediako, D. K., Tunable angle-dependent electrochemistry at twisted bilayer graphene with moire flat bands. *Nature Chemistry* **2022,** *14*, 267-273.
36. Fu, Z.; Hill, J. W.; Parkinson, B.; Hill, C. M.; Tian, J., Layer and material-type dependent photoresponse in $WSe_2/WS_2$ vertical heterostructures. *2D Materials* **2021,** *9* (1).
37.** Tolbert, C. L.; Hill, C. M., Electrochemically probing exciton transport in monolayers of two-dimensional semiconductors. *Faraday Discussions* **2022,** *233*, 163-174.

CG-TC SECCM was used in this study to investigate carrier transport and measure diffusion lengths in monolayer and bilayer $WSe_2$ nanoflakes. Diffusion lengths were measured to be upwards of 20 μm when carriers were generated in a monolayer region, and virtually absent when measured in a bilayer region. This information could not be provided via spectroscopic techniques alone, and shows the power of CG-TC SECCM.

38. Strange, L. E.; Yadav, J.; Garg, S.; Shinde, P. S.; Hill, J. W.; Hill, C. M.; Kung, P.; Pan, S., Investigating the redox properties of two-dimensional $MoS_2$ using photoluminescence spectroelectrochemistry and scanning electrochemical cell microscopy. *Journal of Physical Chemistry Letters* **2020,** *11* (9), 3488-3494.
39. Hill, J. W.; Fu, Z.; Tian, J.; Hill, C. M., Locally engineering and interrogating the photoelectrochemical behavior of defects in transition metal dichalcogenides. *Journal of Physical Chemistry C* **2020,** *124* (31), 17141-17149.
40.** Hill, J. W.; Hill, C. M., Directly mapping photoelectrochemical behavior within individual transition metal dichalcogenide nanosheets. *Nano Letters* **2019,** *19*, 5710-5716.

Topographical information along with electrochemical information provided by SECCM were used to map spatial variations in photoelectrochemical reaction rates in bulk $WSe_2$ nanoflakes. A step-edge height dependent recombination behavior was observed in bulk TMD nanoflakes, where taller step-edges had a larger decrease in outer-sphere redox performance.

41. Zeng, Z.; Yin, Z.; Huang, X.; Li, H.; He, Q.; Lu, G.; Boey, F.; Zhang, H., Single-layer semiconducting nanosheets: High-yield preparation and device fabrication. *Angewandte Chemie* **2011,** *123* (47), 11289-11293.
42. Mak, K. F.; Lee, C.; Hone, J.; Shan, J.; Heinz, T. F., Atomically Thin $MoS_2$: A new direct-gap semiconductor. *Physical Review Letters* **2010,** *105*.
43. Splendiani, A.; Sun, L.; Zhang, Y.; Li, T.; Kim, J.; Chim, C.-Y.; Galli, G.; Wang, F., Emerging photoluminescence in monolayer $MoS_2$. *Nano Letters* **2010,** *10* (4), 1271-1275.
44. Zhao, W.; Ghorannevis, Z.; Chu, L.; Toh, M.; Kloc, C.; Tan, P.-H.; Eda, G., Evolution of electronic structure in atomically-thin sheets of $WS_2$ and $WSe_2$. *ACS Nano* **2013,** *7* (1), 791-797.
45. Bard, A. J.; Fan, F. R. F.; Kwak, J.; Lev, O., Scanning electrochemical microscopy. Introduction and principles. *Analytical Chemistry* **1989,** *61* (2), 132-138.
46. Conzuelo, F.; Sliozberg, K.; Gutkowski, R.; Grutzke, S.; Nebel, M.; Schuhmann, W., High-resolution analysis of photoanodes for water splitting by means of scanning photoelectrochemical micrsocopy. *Analytical Chemistry* **2017,** *89* (2), 1222-1228.
47. Zhao, F.; Plumere, N.; Nowaczyk, M. M.; Ruff, A.; Schuhmann, W.; Conzuelo, F., Interrogation of a PS1-based photocathode by means of scanning photoelectrochemical microscopy. *Small* **2017,** *13* (26).
48. Askarova, G.; Hesari, M.; Wang, C.; Mirkin, M. V., Decoupling through-tip illumination from scanning in nanoscale photo-SECM. *Analytical Chemistry* **2022,** *94* (20), 7169-7173.
49.** Sarkar, S.; Wang, X.; Hesari, M.; Chen, P.; Mirkin, M. V., Scanning electrochemical and photoelectrochemical microscopy on finder grids: Towards correlative multitechnique imaging of surfaces. *Analytical Chemistry* **2021,** *93* (13), 5377-5382.

This study used through-tip illumination SECM in combination with TEM and AFM to show the potential of correlative imaging techniques using $TiO_2$ nanorods as an example particle. This type of multitechnique imaging can be extended into 2DSCs to provide atomic structural information as well as electrochemical information on the same nanoflake to elucidate behavior at active sites.

50. Bae, J. H.; Nepomnyashchii, A. B.; Wang, X.; Potapenko, D. V.; Mirkin, M. V., Photo-scanning electrochemical microscopy on the nanoscale with through-tip illumination. *Analytical Chemistry* **2019,** *91* (20), 12601-12605.
51. Hill, C. M.; Mendoza-Cortes, J. L.; Velazquez, J. M.; Whittaker-Brooks, L., Multi-dimensional designer catalysts for negative emissions science (NES): bridging the gap between synthesis, simulations, and analysis. *iScience* **2022,** *25* (1).